



# Stability And Bearing Capacity Of Strip Footings On Soft Soil Slopes : A Numerical Study Using Plaxis

<sup>1</sup>Anuj Oraon, <sup>2</sup>Abhijit Anand

<sup>1</sup>PG Student , <sup>2</sup>Assistant Professor,

<sup>1,2</sup> Department of Civil Engineering BIT Sindri, Dhanbad, Jharkhand, India

*Abstract:* The primary focus of this research is to analyze the bearing capacity and settlement behavior of strip footings on soft soil slopes. Footings near slope edges are often subjected to different stress distributions due to slope instability. This study simulates the impacts of several types of loads, footing distance from the slope edge, and slope angle using the finite element method (using PLAXIS software). Understanding these factors is crucial for optimizing geotechnical designs, particularly in hilly terrains or near embankments, where stability and bearing capacity are vital concerns.

The bearing capacity of footings is a critical aspect of geotechnical engineering, affecting the stability and safety of structures. Extensive research has been conducted on footings placed on homogeneous soils, but in practice, soils are often layered, with different properties in each layer. Research has focused on improving understanding of alluvial soil slope, especially in without improved layers, impact the bearing capacity and settlement of footings.

**Keywords** - Bearing Capacity, Strip footing, Soil Slope, Soft Soil, Finite Element Method, PLAXIS

## I. INTRODUCTION

Current geotechnical design codes (e.g., IS 6403, Eurocode 7) offer limited provisions for the design of footings on sloping ground, particularly under weak soil conditions, which often results in uncertainties in practical applications. The interaction between footing loads and slope stability is inherently complex, highlighting the need for advanced numerical modeling techniques to achieve reliable assessments. In this study, two-dimensional finite element analysis (PLAXIS 2D) is employed to evaluate the bearing capacity and settlement behavior of strip footings on clayey slopes. Key factors considered include the setback distance of the footing from the slope crest and the shear strength parameters of the soil. The outcomes of this research aim to enhance design approaches and improve the safety and performance of shallow foundations constructed on slopes.

Strip footings are one of the most widely used shallow foundation systems in civil engineering, particularly for supporting load-bearing walls and columns in residential, commercial, and low- to medium-rise buildings. Their primary function is to distribute the structural loads from superstructures evenly to the underlying soil, ensuring stability and preventing excessive settlement. Strip footings are especially effective in soils with adequate bearing capacity near the surface, making them economical and straightforward to construct. In sloped terrains and soft soil conditions, understanding the behavior of strip footings becomes crucial, as improper design can lead to differential settlement or failure. Moreover, due to their linear and continuous nature, strip footings are well-suited to resist moderate horizontal loads and accommodate moderate changes in soil bearing properties along their length. Their importance is further emphasized in geotechnical research and practice due to their influence on overall structural performance, making them a critical element in both traditional and modern foundation engineering.

Soft soils are commonly encountered in many parts of the world, especially in coastal areas, riverbanks, and alluvial plains. These soils are characterized by low shear strength, high compressibility, and poor load-bearing capacity. Foundations constructed on such soils often face challenges such as excessive settlement, reduced bearing capacity, and potential instability, especially when situated near or on slopes.

The primary objective of this thesis is to employ the finite element method (FEM) for a numerical parametric investigation aimed at evaluating the bearing capacity and failure mechanisms of a strip footing placed on a  $c-\phi$  soil slope. This study specifically aims to:

- Quantify the effects of various geometric and soil strength parameters on the bearing capacity of strip footings nearby slopes.
- Compare numerical results with classical bearing capacity theories (e.g., Terzaghi)
- Evaluate how slope geometry and soil properties influence the failure mechanism.
- To evaluate the factor of safety (FoS) of soil slopes using PLAXIS simulations.

## II. METHODOLOGY

### 2.1 Experimental Work

#### A. Material

**Alluvial Soil:** The soil sample used in this study was collected from an alluvial deposit located approximately three kilometers away from BIT Sindri, within the Damodar River basin in Dhanbad.

#### Soil

The soil used in this study is an Organic soil (OH) collected from a river basin of Damodar River. The soil was transported to BIT Sindri's Soil Mechanics Laboratory, where it was spread on the floor to dry naturally before being rammed into smaller sizes. The pit from where the soil was obtained is shown in fig. 1



**Fig. 1.** Pit from where soil was collected

#### B. Methods

*The following Indian standard codes were followed during the study's execution*

1. IS:2720(Part 4):1985 Grain Size Analysis by Wet Sieving
2. IS:2720 (Part 3): 1980 Specific Gravity test of Soil using Pycnometer
3. IS:2720 (Part 5): 1985 Atterberg Limit Test for Liquid and Plastic Limits
4. IS:2720(Part 7): 1980 Standard Proctor Test (Compaction)

#### C. Grain Size Distribution by Wet Sieving

- A 500 g oven-dried soil sample is taken and soaked in clean water to disintegrate any clay lumps and loosen fine particles.
- The sample is thoroughly stirred and allowed to soak for a minimum of 10 minutes.
- The suspension is then poured through a 75  $\mu\text{m}$  sieve, allowing particles finer than this size to pass through.

- The washing is continued with water until the effluent becomes clear, indicating that all fines have been removed.
- The soil retained on 75  $\mu\text{m}$  sieve was carefully collected and subsequently oven-dried.
- The dried material is then subjected to dry sieve analysis using a mechanical sieve shaker for 10 minutes.
- The material retained on each sieve is collected and weighed individually to determine the grain size distribution.

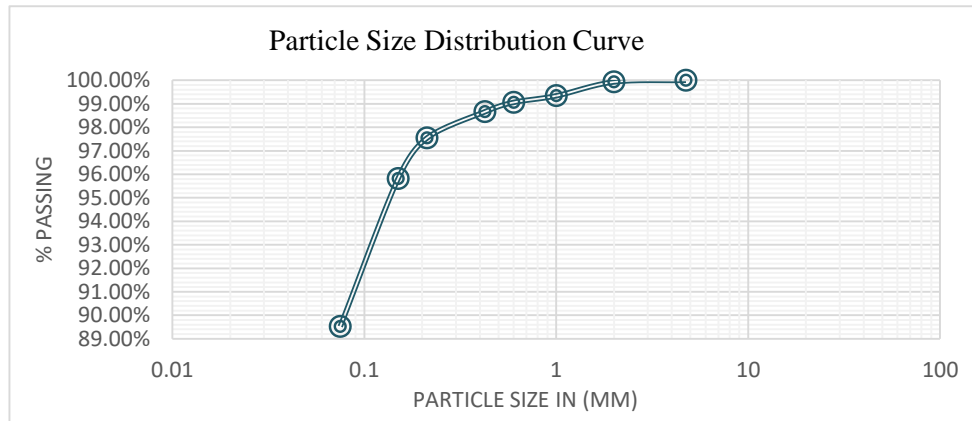


**Fig. 2.** Particle Size Distribution Curve

#### D. Specific Gravity Test of Soil Using Pycnometer

##### *Apparatus Description*

A pycnometer is a glass bottle with a capacity of approximately 900 mL, fitted with a brass screw-top lid containing a small central hole to allow the escape of air. The pycnometer method is suitable for determining the specific gravity of both fine-grained and coarse-grained soils.

##### *Procedure*

Before commencing the test, the pycnometer is thoroughly cleaned and dried to ensure accurate measurements. The following steps are carried out:

- The mass of the empty pycnometer is recorded.
- A known quantity of oven-dried soil sample is added to the pycnometer, and the combined weight is measured.
- The pycnometer is then filled with distilled water until it reaches approximately half of its height, and the mixture is stirred thoroughly to start the mixing process.

##### *Air Removal and Final Filling*

To eliminate entrapped air bubbles, additional water is added, and the mixture is stirred once again. After ensuring complete mixing, the screw cap is securely fastened, and distilled water is added through the top hole until the pycnometer is completely filled. Any excess water is wiped off, and the final weight of the pycnometer with the soil-water mixture is recorded.



**Fig. 3:** Pycnometer

**E. Standard Proctor Test**

The compaction characteristics of the soil specimen were determined in accordance with IS: 2720 (Part 7) – 1980, which specifies the procedure for evaluating moisture content and dry density using the standard Proctor (light compaction) method. This test is fundamental in geotechnical investigations as it provides reliable measurements of soil properties necessary for analysis and design. The compaction results further establish the relationship between moisture content and dry density, enabling the identification of the optimum moisture content and maximum dry density.

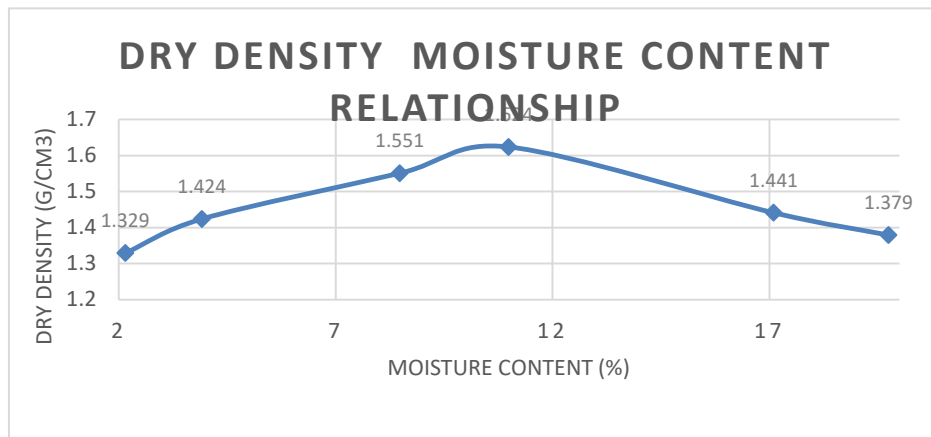


**Fig. 4.** Dry Density Moisture Content Relationship

**Table 2.1.** Specifications of natural soil .

Properties	Values
Specific Gravity	2.2
Liquid Limit	26
Optimum Moisture Content (%)	10.99
Dry Density (g/cm <sup>3</sup> )	1.624
Maximum dry density ( $\gamma_d$ ) (kN/m <sup>3</sup> )	15.93
Saturated unit weight ( $\gamma_{sat}$ ) (kN/m <sup>3</sup> )	18.53
Plastic Limit	19.80
Plastic Index (%)	6.2

### III. MODELING AND ANALYSIS

#### 3.1 Numerical Modelling

##### *Finite Element Method*

To validate the findings of laboratory model tests and to examine the internal deformation mechanisms within the soil, a series of two-dimensional finite element method (FEM) was conducted on a prototype footing–slope system. Numerical modeling was carried out using PLAXIS 2D, a geotechnical finite element software developed by Brinkgreve and Vermeer (2002), which is widely recognized for its reliability in simulating complex soil–structure interactions. By replicating the experimental setup computationally, the study aimed to achieve a deeper understanding of stress distribution, potential failure mechanisms, and the load–deformation response of the footing.

This study utilizes finite element method (FEM) in PLAXIS 2D to examine the bearing capacity of strip footings placed on sloping ground and to evaluate slope stability under varying loading conditions. The numerical simulations are carried out using a plane strain approach, which provides a reliable representation of the two-dimensional soil–footing interaction. The soil behavior is modeled using the Mohr–Coulomb failure criterion, characterized by an elastic–perfectly plastic response, enabling the analysis to capture the transition from elastic deformation to plastic failure with sufficient accuracy.

The analysis builds upon the findings of Acharyya and Dey [1], who demonstrated through finite element analysis that variations in soil elastic modulus have minimal influence on footing bearing capacity when placed on slopes. Based on this conclusion, a constant Young's modulus value was maintained across all simulations. The concrete footing, with a specified thickness of 0.5 m, was represented in PLAXIS 2D using plate elements characterized by: Flexural stiffness ( $EI = 2.92 \times 10^5 \text{ kN}\cdot\text{m}^2/\text{m}$ ) Axial stiffness ( $EA = 1.4 \times 10^7 \text{ kN/m}$ ). The software's automatic boundary condition assignment feature was utilized, applying: Full fixity (both horizontal and vertical constraints) at the model base.

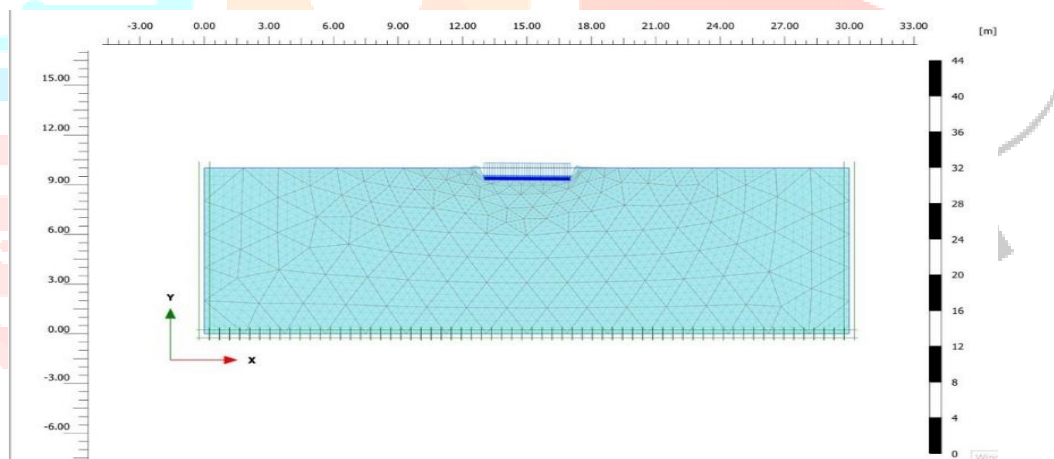


**Fig. 5.** A numerical model was developed in PLAXIS 2D to simulate the behavior of a footing on a horizontal ground surface.

Horizontal restraints only at the vertical boundaries sensitivity analyses verified that these boundary conditions did not introduce artificial constraints affecting the solution accuracy. For discretization, the study employed: 15-noded triangular elements Medium-density mesh configuration . Local refinement near the footing-slope interface.

##### **Boundary Conditions**

The lateral boundaries of the numerical model were restrained against horizontal displacement, while the bottom boundary was fixed in both the horizontal and vertical directions to prevent rigid body motion. The strip footing was idealized as a rigid element and positioned at varying setback distances from the slope crest to evaluate its influence on bearing capacity and deformation behavior.

Plaxis 2D model setup

Geometry :

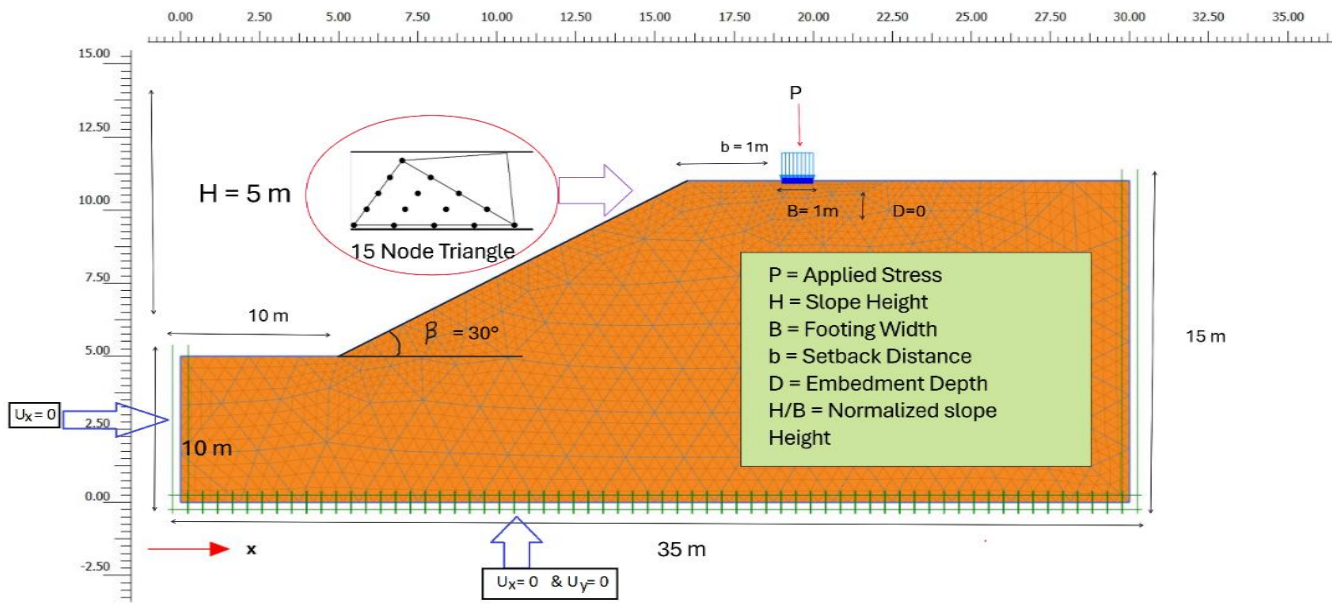
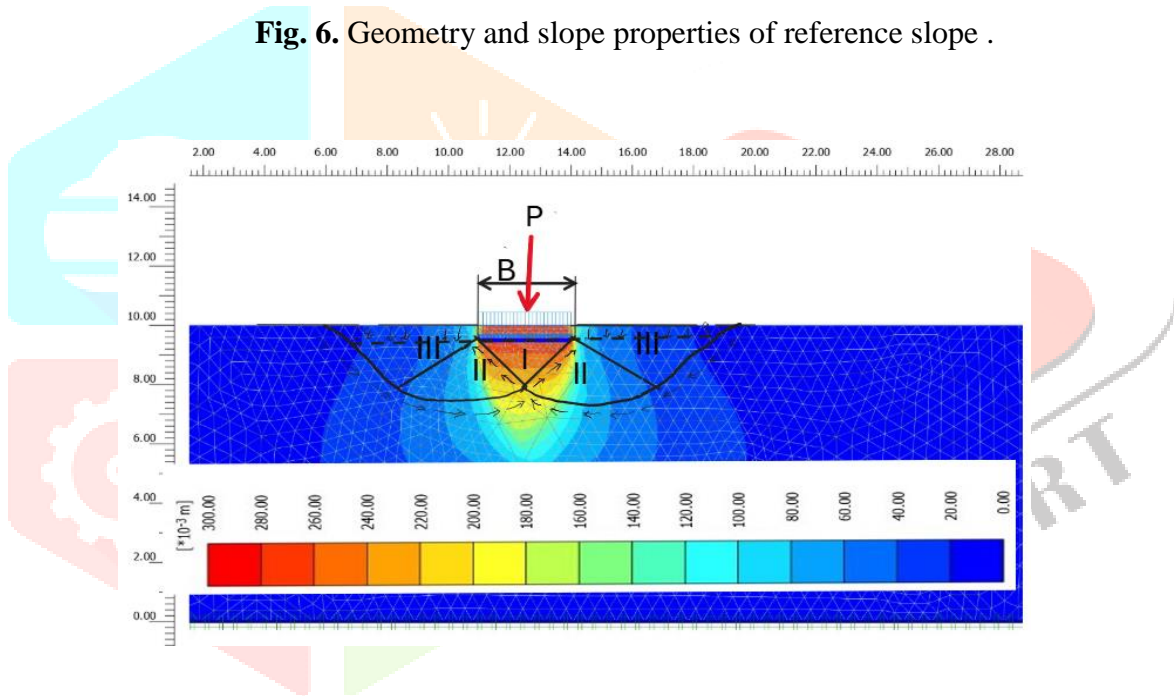


Fig. 6. Geometry and slope properties of reference slope .



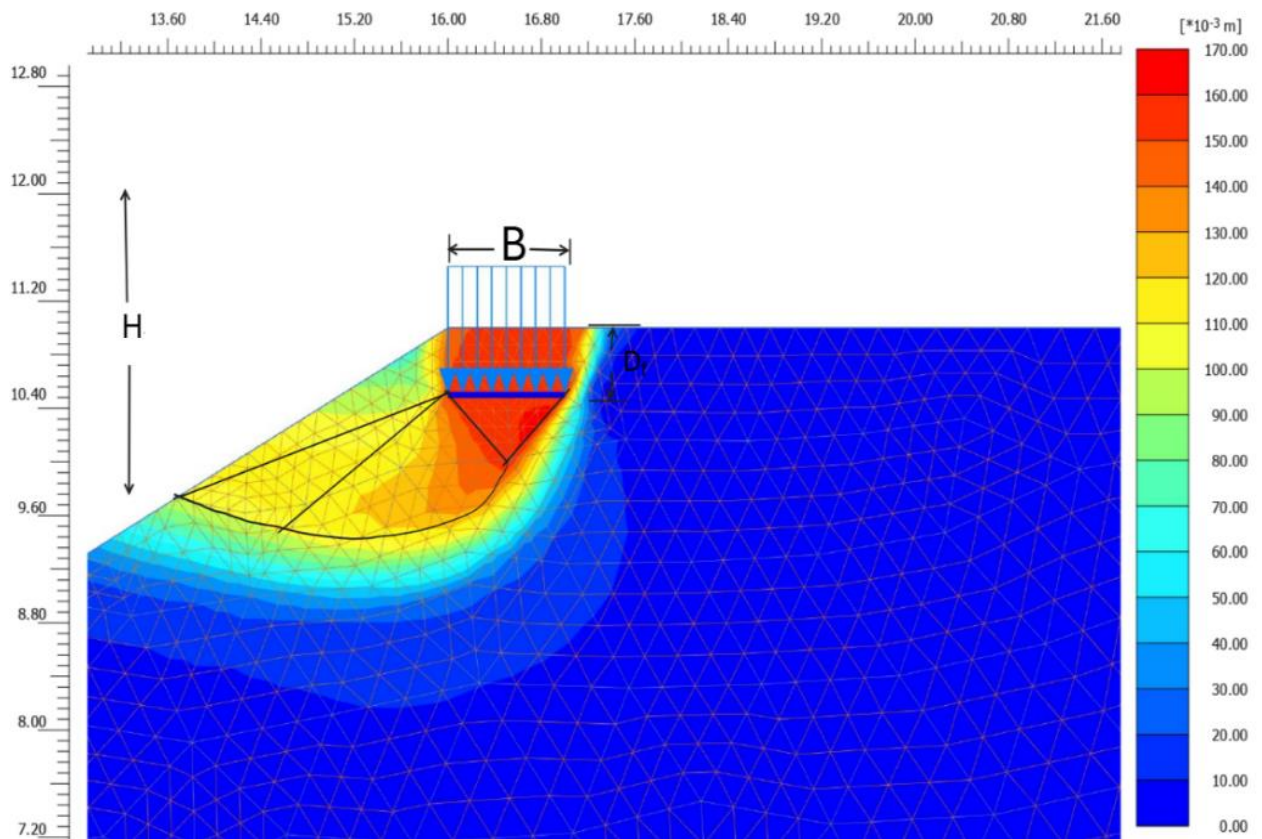
*Terzaghi s Bearing Capacity Theory*

- I. SOIL WEDGE UNDER FOOTING
- II. PLASTIC ZONE
- III. PASSIVE ZONE

Fig. 7. Terzaghi system for ideal soil , rough base and surcharge

Ultimate Bearing capacity of strip footing is given by the equation :

$$Q_u = CN_c + \gamma D N_q + 0.5\gamma B N_\gamma \tag{1}$$



- I. CENTRAL ZONE
- II. RADIAL SHEAR ZONE
- III. LINEAR SHEAR ZONE

**Fig. 8.** Development of plastic zones and potential slip surfaces in the vicinity of a rough strip footing positioned at the crest of a slope.

**Table 3.1.** Specifications of natural soil

Parameter	unit	Values
Footing setback distance (b/B)	-	0,1,2,3,4,5,7
Slope angle ( $\beta$ )	-	30,40 ,50
Footing Width (B)	m	1,2,3,4,5
Slope Height Ratio	m	5,7,9
Factor of Safety	m	1.82

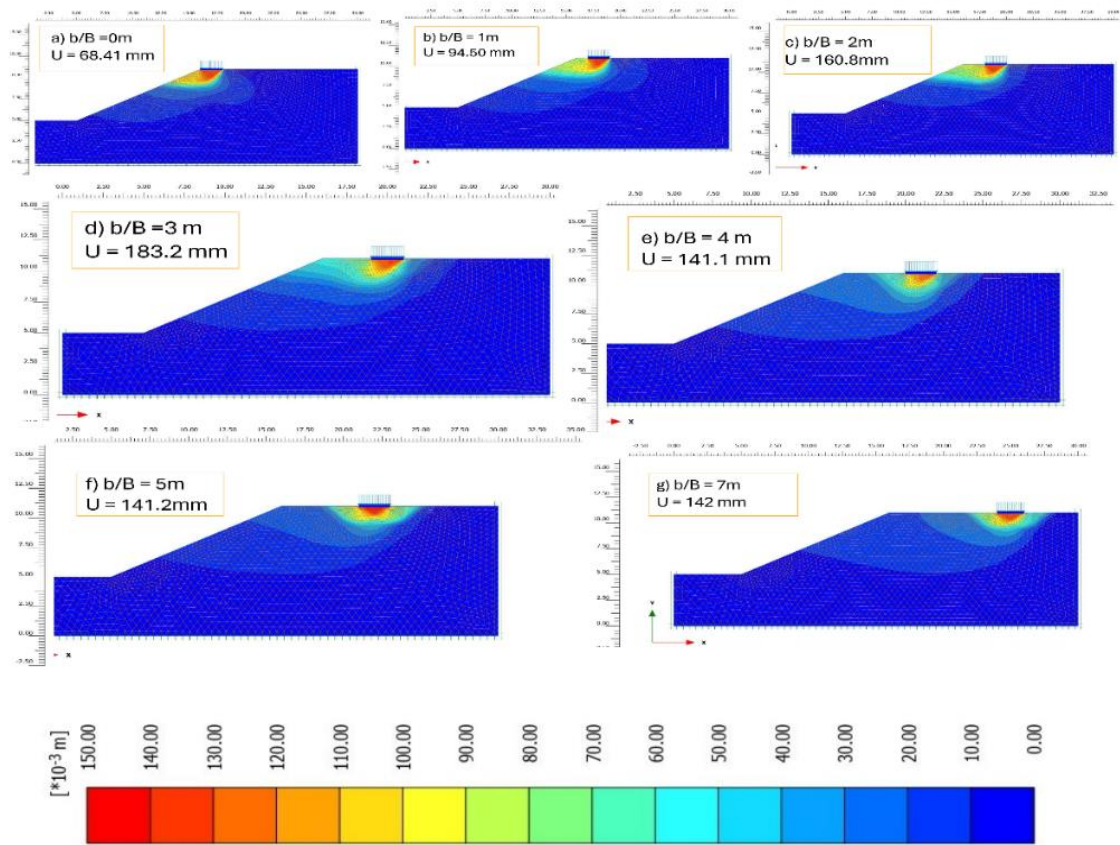


Fig. 9. “Variation in the failure surface for footings of different widths (B) at a constant setback distance (b)

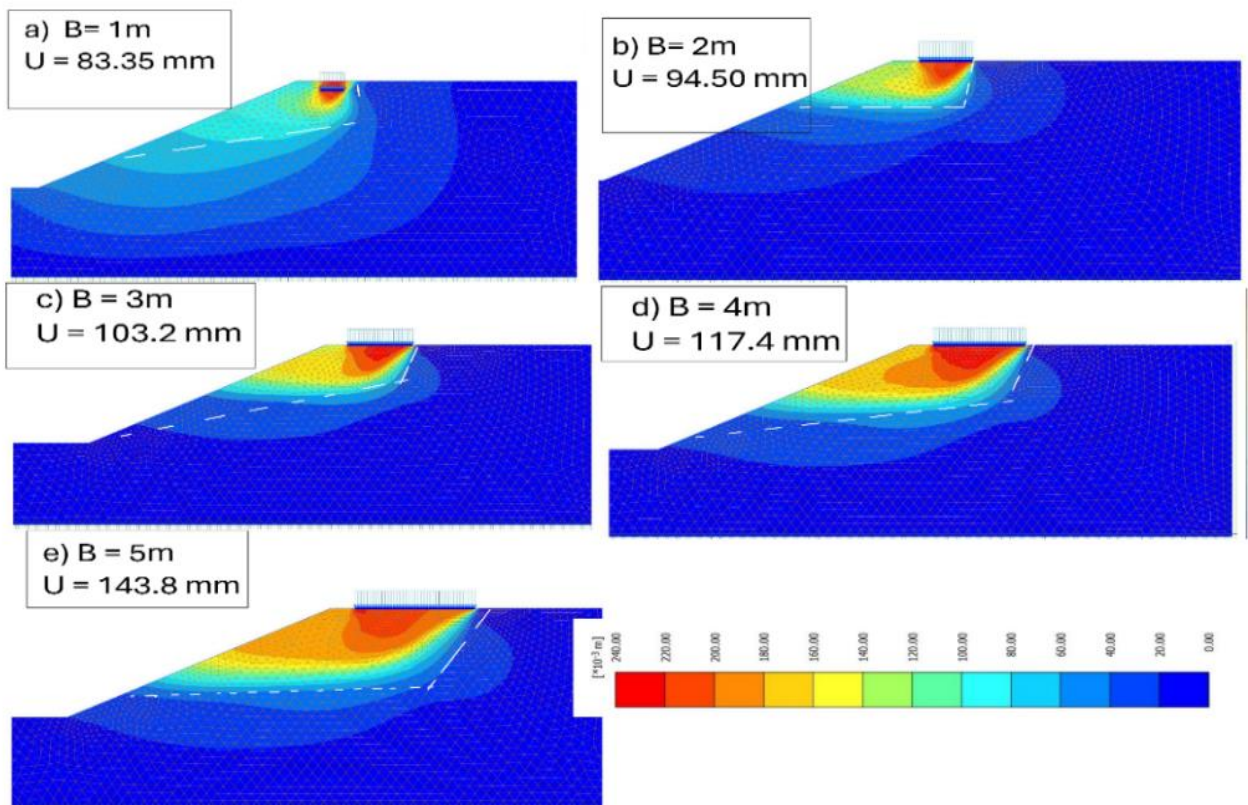
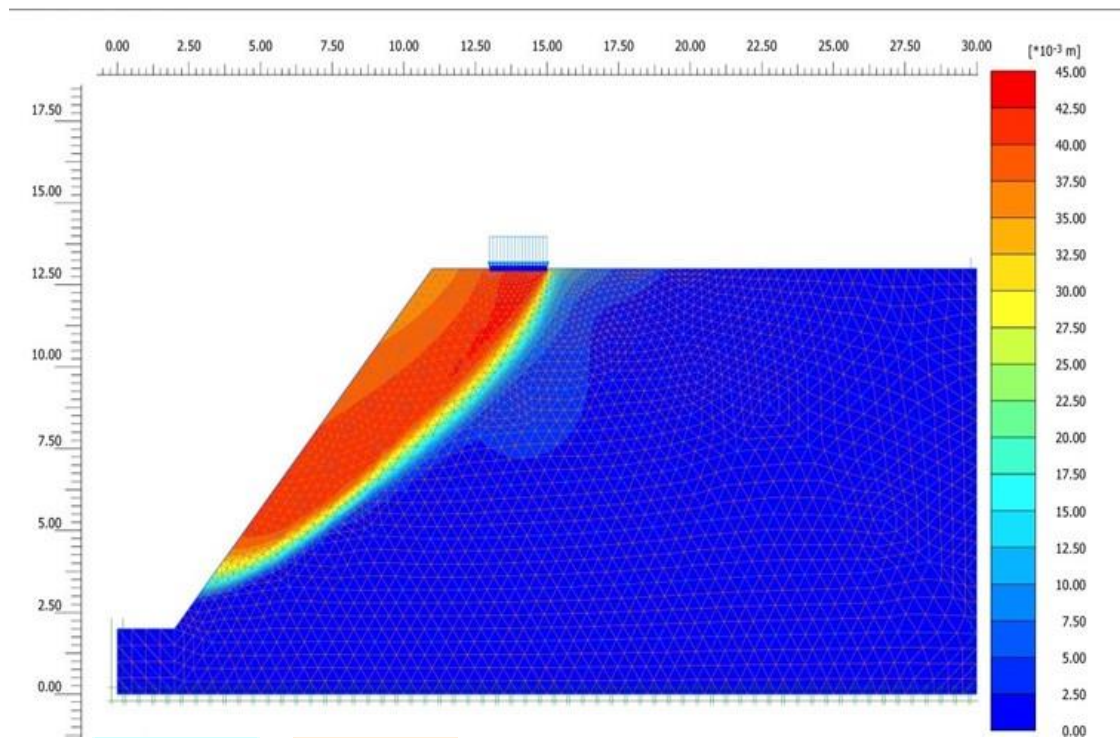
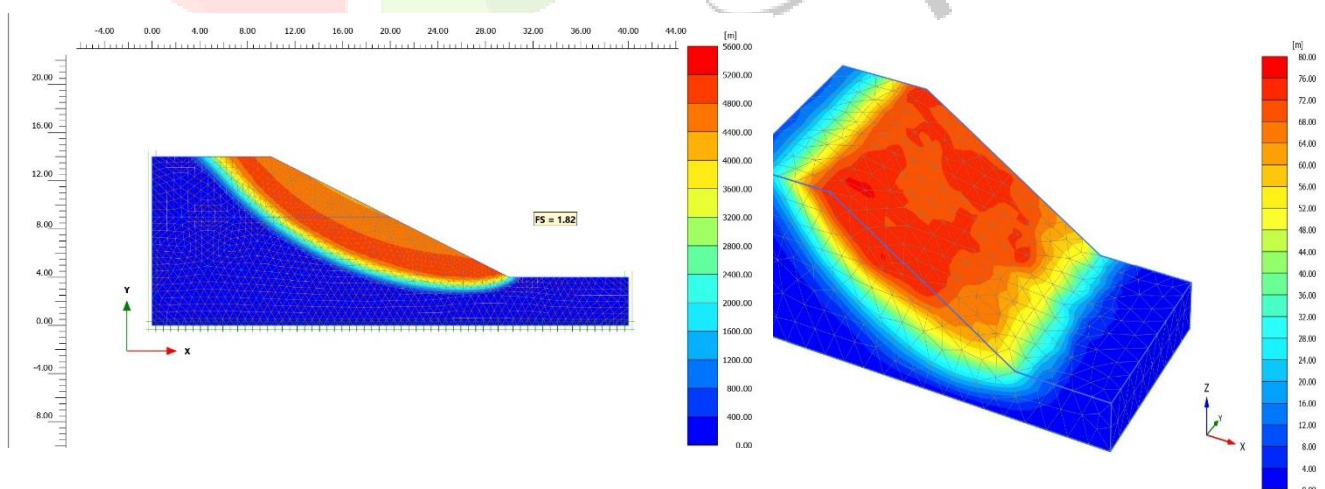


Fig. 10. “Variation in the failure surface for footings of different widths (B) at a constant setback distance (b)



**Fig. 11.** Influence of slope height (H) on the development of the failure surface at a given slope angle ( $\beta$ )

Foundations on sloped terrain present unique geotechnical challenges due to the reduced passive resistance and the potential for slope failure. Understanding the relationship between slope geometry and footing behavior is essential for safe design. In this context, numerical modeling provides a powerful tool for evaluating soil structure interaction under complex slope conditions. This study focuses on analyzing the effect of varying slope angles and h/b ratios on the bearing capacity of a strip footing using PLAXIS 2D software. The findings are used to understand how the slope steepness and slope height relative to footing width influence footing performance.



**Fig. 12.** Influence of Factor of Safety Obtained from finite element method

Slope stability is of paramount importance in geotechnical engineering projects involving embankments, natural slopes, and excavations. The stability of a slope is typically quantified by its Factor of Safety (FOS), which represents the ratio of resisting forces to driving forces. Advanced numerical techniques such as finite element modeling (FEM) allow for more accurate predictions of slope behavior under various loading scenarios.

### IV. RESULTS AND DISCUSSION

4.1 The load-settlement curves for the three loading scenarios are plotted on a common graph (see Fig. 13.). Each curve shows a nonlinear increase in settlement with load, typical for soft soils. The settlement increases rapidly after a certain load threshold, indicating local shear failure.

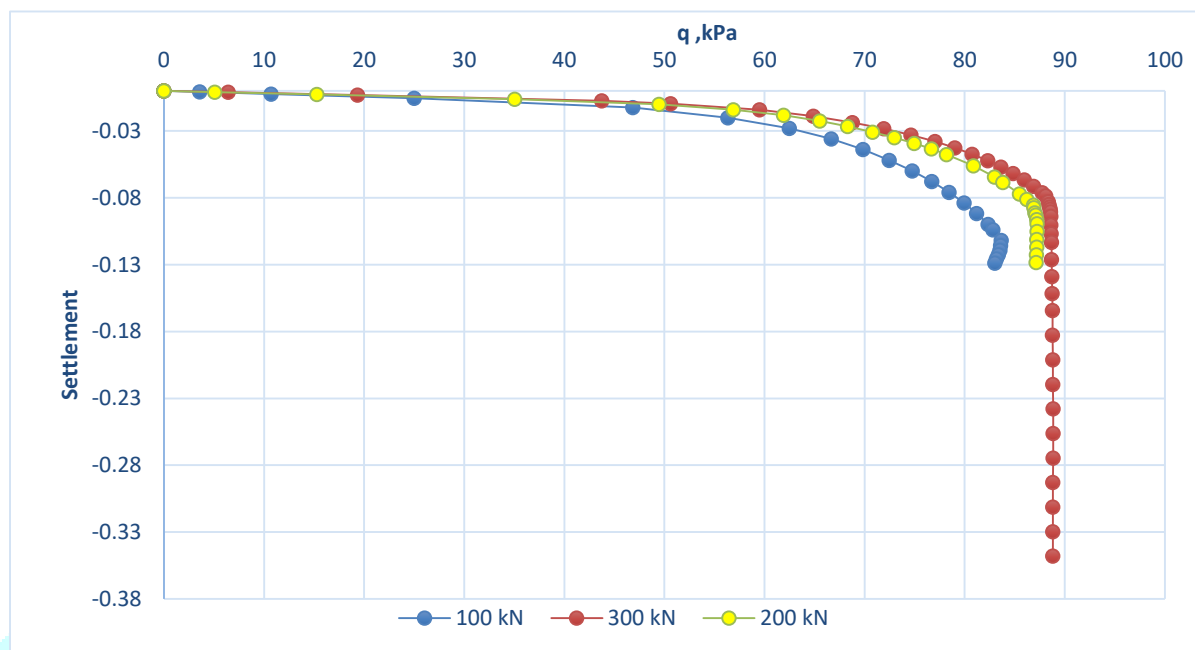


**Fig. 13.** Load–settlement response for different 3b/B ratios obtained from model tests on slopes .

For all load levels, the initial portion of the curve is nearly linear, representing the elastic behavior of the soil.

Beyond a certain load, a rapid increase in settlement occurs, indicating plastic deformation and soil yielding.

The 300 kN curve shows a long plastic zone, suggesting failure is approached or achieved.

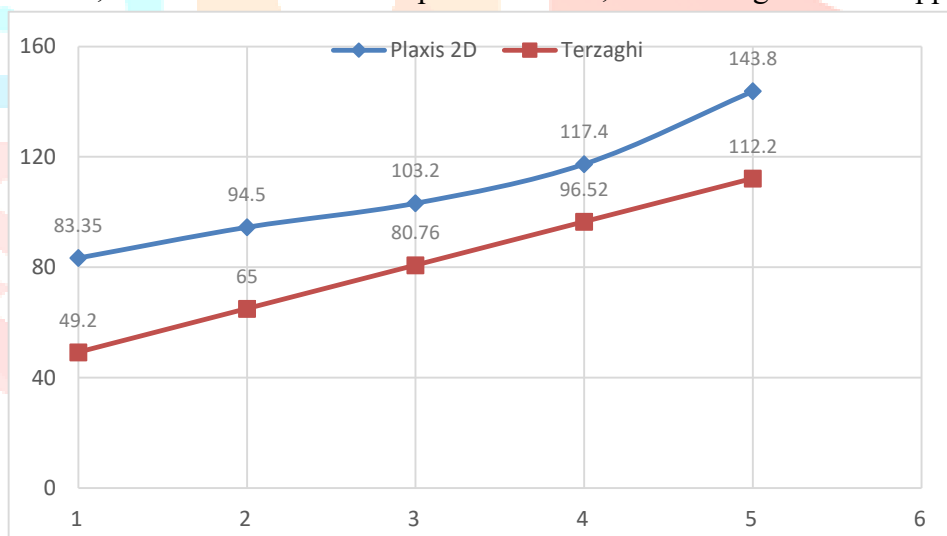
**Table 4.1.** Comparative behavior across load cases.

Parameters	100 kg Load	200 kg load	300 kg load
<b>Initial Settlement</b>	0.001m	0.001m	0.001m
<b>Settlement at 80 kN</b>	0.09	0.10	0.11
<b>Max Settlement</b>	0.13	0.13	>0.34
<b>Failure Observed</b>	No	Borderline	Yes
<b>Stiffness loss</b>	Moderate	High	Severe



**Fig. 14.** Relationship between ultimate bearing capacity and footing setback ratio (b/B).

When the footing was placed too close to the slope, both bearing capacity and settlement performance degraded. For  $b/B \geq 4$ , the influence of the slope diminished, and footing behavior approached that on



level ground.

**Fig. 15.** Variation in the failure surface of footings with different widths (B) at a constant setback distance (b).

## 4.2 Observed Trends

### PLAXIS 2D Results:

1. Show a nonlinear increase in bearing capacity with footing width.
2. Suggest that as the width increases, the failure surface becomes wider and deeper, mobilizing more soil strength.
3. PLAXIS considers actual deformation, stress redistribution, and plastic flow, resulting in more realistic predictions.

### Terzaghi's Theory:

1. Also shows increasing trend but at a much lower rate.
2. Uses a simplified model based on assumed failure surfaces (log-spiral and Rankine zones).

3. Tends to underpredict capacity, especially for wider footings, due to the lack of stress interaction modeling.

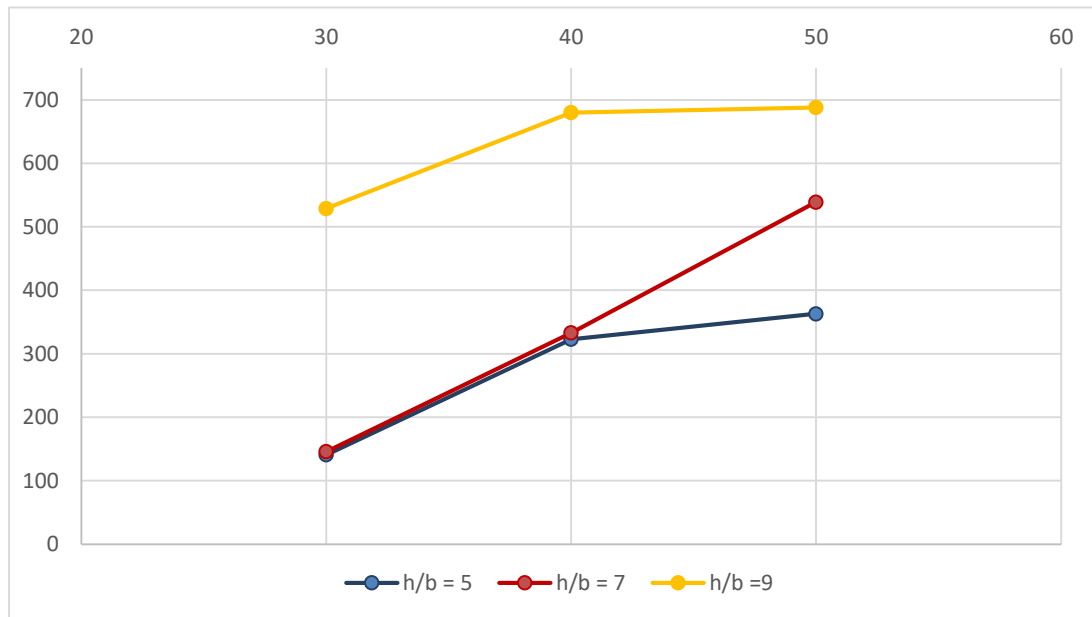


**Fig. 16.** Slope angle,  $\beta$  (deg.)

The results obtained from PLAXIS 2D simulations are plotted as shown in the graph. The y-axis represents ultimate bearing capacity (in kN/m), and the x-axis shows the slope angle in degrees.

#### 4.3 Effect of Slope Angle

- For all values of the height-to-width ( $h/b$ ) ratio, the bearing capacity tends to stabilize as the slope angle increases because bearing capacity decreases as slope angle increases.
- Steeper slopes ( $50^\circ$ ) reduce stability, limiting the soil's ability to resist vertical loads.

#### 4.4 Effect of $h/b$ Ratio

At each slope angle:

- $h/b = 9$  consistently yields the highest bearing capacity, indicating a deeper and more stable slope.
- $h/b = 5$  gives the lowest capacity, particularly at lowest slope angles ( $30^\circ$ ).

#### 4.5 Interaction Effects

For  $h/b = 5$ , the increase in slope angle from  $40^\circ$  to  $50^\circ$  leads to a moderate rise in bearing capacity

For  $h/b = 7$ , the increase is more pronounced—particularly at  $50^\circ$ , the bearing capacity reaches over 539 kN/m.

For  $h/b = 9$ , bearing capacity is highest at all slope angles, reaching around 688 kN/m at  $50^\circ$ , showing that greater slope height contributes positively by engaging more soil mass in resisting loads.

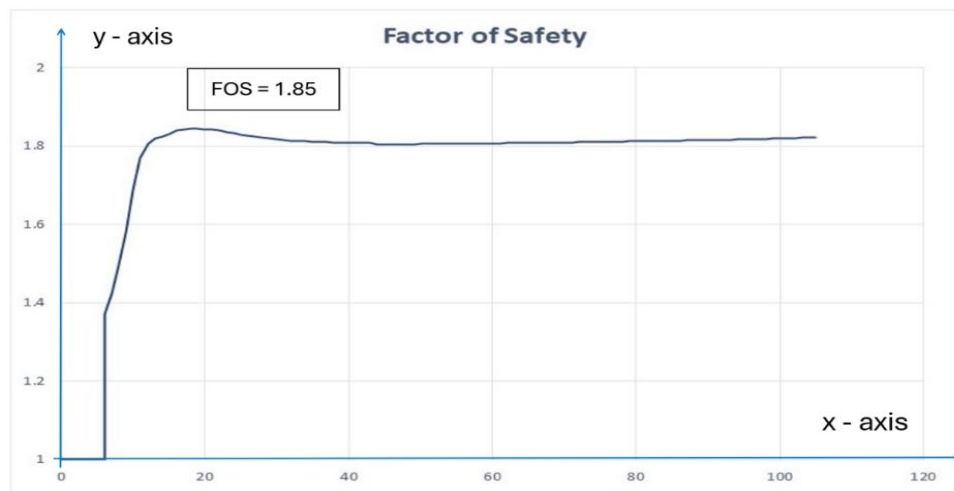


**Fig. 17.** Graph of factor of Safety obtained from FEM .

Initially, the slope showed low stability ( $FOS \approx 1.0$ ), representing conditions close to failure.

As staged construction or loading was applied, the slope's FOS rapidly increased, peaking at around 1.85.

The curve then slightly declined and stabilized, fluctuating minimally around 1.80 through the remaining load steps, indicating achieved slope stability.

## CONCLUSION

The ultimate load-carrying capacity of the soil–foundation system was evaluated to fall between 83 and 88 kN/m, with variations governed by the applied loading level and the geometric characteristics of the footing–slope arrangement. Examination of the load–settlement response showed that applied loads of 100 kg and 200 kg produced settlements within acceptable serviceability limits. However, when the applied load reached 300 kg, the footing experienced excessive settlement exceeding 0.3 m, clearly indicating the occurrence of bearing failure. The gradual increase in settlement with increasing load demonstrates the progression of soil behavior from an elastic response to plastic deformation, highlighting the need for conservative safety considerations in foundation design.

The analysis further revealed that the bearing resistance of strip footings constructed near slopes improves noticeably with an increase in the setback distance ( $b$ ) from the slope crest. The most unfavorable bearing conditions were observed when the footing was located directly at the edge of the slope, which can be attributed to concentrated stresses and the heightened likelihood of slope-related instability. As the footing was positioned farther away from the crest, it moved beyond the critical failure zone, resulting in enhanced stability and increased resistance of the supporting soil. When the setback distance reached 4 m or more, the effect of the slope on footing performance became negligible, and the response closely matched that of a footing founded on horizontal ground. These observations confirm the importance of the setback ratio ( $b/B$ ) as a governing parameter in the design of foundations near sloping terrain.

Results obtained from PLAXIS 2D numerical simulations indicated a more substantial increase in ultimate bearing capacity with increasing footing width compared to estimates derived from Terzaghi's classical analytical approach. Although Terzaghi's method is suitable for preliminary evaluations, it consistently yielded lower bearing capacity values, particularly for wider footings and cases involving complex stress redistribution. This underestimation arises from the simplified assumptions underlying Terzaghi's formulation, which does not fully represent nonlinear soil behavior, anisotropic conditions, or realistic failure mechanisms.

In addition, an increase in the embedment ratio ( $h/B$ ) was found to significantly improve foundation stability and load-bearing performance due to enhanced confinement of the surrounding soil. Conversely, steeper slope inclinations led to a reduction in bearing capacity as a result of diminished lateral support and increased shear demand within the soil mass. The slope stability assessment produced a Factor of Safety of approximately 1.8, confirming that the modeled slope remained stable under the analyzed conditions. The observed stabilization pattern—characterized by an initial rapid increase followed by steady equilibrium—reflects appropriate slope geometry and sound analytical assumptions.

Overall, the findings demonstrate that advanced numerical modeling tools such as PLAXIS 2D provide a robust and reliable framework for analyzing soil–structure interaction and for optimizing the design of strip footings constructed on or near slopes under diverse loading and geometric scenarios.

## REFERENCES

- [1] Abhijit Anand and Rajib Sarkar. (2021). A comprehensive study on bearing behavior of cement–fly ash composites through experimental and probabilistic investigations. *International Journal of Geo-Engineering*.
- [2] Acharyya, R. (2019). Finite element investigation and ANN-based prediction of the bearing capacity of strip footings resting on sloping ground. *International Journal of Geo-Engineering*.
- [3] Alammyan, A. A. (2021). *Bearing capacity and failure mechanism of shallow footings on unreinforced slopes: a state-of-the-art review*. International Journal of Geotechnical Engineering.
- [4] Al-Baghdadi, W. M. (2010). Analysis of strip footings resting on reinforced granular trench by the finite element method. *International Journal of Geotechnical Engineering*, 471-482.
- [5] Altalhe, E. B. (2015). Behavior of strip footing on reinforced sand slope. *Journal of Civil Engineering and Management*, 10.3846/13923730.2014.890646-18223605.
- [6] Anand, A. (2020). Probabilistic Investigation on Bearing Capacity of Unsaturated Fly Ash. *Journal of Hazardous, Toxic, and Radioactive Waste*, 2153-5493.
- [7] El Sawwaf, M. A. (2007). Behavior of strip footing on geogrid-reinforced sand over a soft clay slope. *Geotextiles and Geomembranes*, 50-60.
- [8] El Sawwaf, M. A. (2012). Cyclic settlement behavior of strip footings resting on reinforced layered sand slope. *Journal of Advanced Research*, 20901232.
- [9] El-Emam, M. (2023). Bearing capacity of strip footing on top of slope: Numerical parametric study. *Ain Shams Engineering Journal*.
- [10] Haghbin, M. (2016). Bearing capacity of strip footings resting on granular soil overlying soft clay. *International Journal of Civil Engineering*, 23833874.
- [11] Miraei, S. (2020). Tunnelling-induced deformation and damage on framed structures with masonry infills.
- [12] Naeini, S. A. (2012). Bearing capacity and settlement of strip footing on geosynthetic reinforced clayey slopes. *Journal of Central South University of Technology (English Edition)*, 10059784.
- [13] Raj, D. (2013). BEARING CAPACITY OF SHALLOW FOUNDATION ON SLOPE: A REVIEW Bearing Capacity of Shallow Foundation on Slopes